Guanidinium-Stapled Helical Peptides for Targeting Protein-Protein Interactions

Camille Perdriau, Anaïs Luton, Katharina Zimmeter, Maxime Neuville, Claire Saragaglia, Carole Peluso-Iltis, Judit Osz, Brice Kauffmann, Gavin Collie, Natacha Rochel, et al.

How to cite: *Angew. Chem. Int. Ed.* **2025**, *64*, e202416348
doi.org/10.1002/anie.202416348

Peptides

Guanidinium-Stapled Helical Peptides for Targeting Protein-Protein Interactions

Camille Perdriau, Anaïs Luton, Katharina Zimmeter, Maxime Neuville, Claire Saragaglia, Carole Peluso-Iltis, Judit Osz, Brice Kauffmann, Gavin W. Collie, Natacha Rochel, Gilles Guichard, and Morgane Pasco**

Abstract: Peptide stapling has emerged as a versatile approach in drug discovery to reinforce secondary structure elements especially α-helices and improve properties of linear bioactive peptides. Inspired by the prevalence of arginine in protein-protein and protein-DNA interfaces, we investigated guanidinium-stapling as a means to constrain helical peptides. Guanidinium stapling was readily achieved on solid support, utilizing two orthogonally protected lysine or unatural α-amino acid residues with an amino function. This method allows for easy modulation of the nature and size of the staple as well as helix propensity. Evaluating a set of guanidinium-stapled peptides for their interaction with different protein targets identified several binders with increased target affinity. X-ray structure determination of four complexes revealed that all stapled peptides adopt a helical conformation upon protein binding. Notably, the disubstituted guanidinium generally exhibits a distinct *cis*/*trans* conformation and, in one instance, retains a conserved hydrogen bond with the protein surface. By identifying, for the first time, the guanidinium moiety as an effective helical peptide stapling group, this research significantly expands the repertoire of α-helix stapling techniques for the creation of useful protein mimics.

Introduction

Macrocyclization stands out as one of the most advanced contemporary strategies to enhance the potential of natural α-peptides, overcome some of their limitations and convert them into valuable pharmacological tools or drugs.[1] Macrocyclization allows the stabilization of peptide bioactive conformation and to mimic structured regions of proteins[2] – e.g. helices – involved in protein-protein interactions (PPI) or recognition of nucleic acids, and doing so decrease the entropic cost associated with peptide binding to the target of interest. Moreover, cyclic peptides can display enhanced properties such as selectivity for the target, improved metabolic stability and prolonged duration of action compared to the cognate linear peptides. Many methodologies have been developed to generate cyclic peptides, by connecting their backbone atoms and/or side chains either directly or through the use of external multifunctional crosslinks.[3] Notably, certain biorthogonal techniques within this spectrum hold promise for the generation of genetically encoded cyclic peptide libraries.[4]

Most popular side chain crosslinking – 'stapling' – strategies such as those based on cysteine with the formation of thioether and bisthioether bridges,[4a,b,5] lactamization,[6] 1,3-dipolar cycloaddition,[7] S_NAr N-arylation,[8] and olefin ring closing metathesis[9] have found widespread applications in the context of α-helix mimicry to rigidify the helical peptide backbone (Figure 1a).[2] It is commonly accepted that depending on the peptide sequence, the nature and the position of the staple may directly and positively contribute to the interaction with the protein surface.[10] It may also influence other properties such as aqueous solubility and cellular uptake,[11] the hydrophobic surface area of the staple being an important parameter.[12] A substantial number of bioactive, cell permeable stapled peptide inhibitors have been reported, yet directing stapled peptides to the cytosol or the nucleus remains a challenge when targeting intra-

[*] Dr. C. Perdriau, A. Luton, K. Zimmeter, Dr. M. Neuville, C. Saragaglia, Dr. G. Guichard, Dr. M. Pasco
Univ. Bordeaux, CNRS, Bordeaux INP, CBMN, UMR5248, IECB, 2 rue Robert Escarpit, F-33600, Pessac, France
E-mail: g.guichard@iecb.u-bordeaux.fr
m.pasco@iecb.u-bordeaux.fr

Dr. M. Neuville
IMMUPHARMA BIOTECH SAS, 15 rue de Bruxelles, 75009 Paris, France

C. Peluso-Iltis, Dr. J. Osz, Dr. N. Rochel
Institut de Génétique et de Biologie Moléculaire et Cellulaire (IGBMC), INSERM, U1258/CNRS, UMR 7104/Univ. Strasbourg 67404 Illkirch (France)

Dr. B. Kauffmann
Univ. Bordeaux, CNRS, INSERM, IECB, UAR3033, US001, F-33600, Pessac (France)

Dr. G. W. Collie
Discovery Sciences, R&D, AstraZeneca, Cambridge, CB2 0AA (UK)

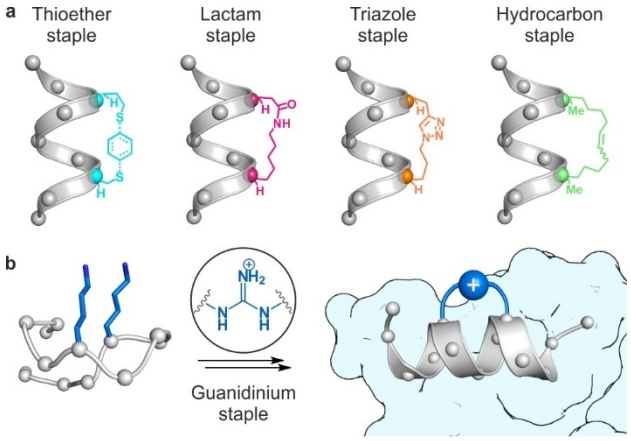

Figure 1. (a) Some classical stapled peptides found in the literature. (b) General Scheme of our guanidinium stapling strategy stabilizing peptides in their bioactive conformation and yielding a positively charged crosslink.

cellular proteins, and further charge optimization of the peptide sequence is often required.[13,14]

In this work, we aimed to combine the stabilization of secondary structure motifs with the introduction of a positive charge through a guanidinium moiety directly incorporated into the hydrocarbon staple (Figure 1b).

Our approach is further motivated by the abundance of guanidinium side chains (Arg residues) in protein-protein binding interfaces and their involvement in a broad spectrum of interactions ranging from H-bonding, ion pairing to cation-π interactions.[15] Thus, in addition of adding a positive charge to the molecule, the guanidinium staple could contribute favorably to specific interactions with the protein surface via the intracyclic guanidinium as well as through the adjacent methylene groups (via Van der Waals contacts) and be used as a constrained Arg residue mimic. The advantages of the approach are that guanidinium crosslinks would be (*i*) synthetically accessible from Lys and any other (un)natural α-amino acid residues with alkyl amine side chains (ornithine (Orn), diaminobutyric acid (Dab),…) to modulate the ring size, and (*ii*) formed selectively on-resin using standard synthetic methods.[16] Only a few attempts to incorporate a guanidinium moiety into cyclic peptides have been reported,[17] and to our knowledge, there is no information about the ability of these staples to introduce helix-inducing constraints. Moreover, guanidinium staples have not yet been applied to design peptide inhibitors of protein-protein interactions and no high-resolution structural information is currently available. Here, we describe an optimized and robust solid-phase synthesis (SPS) method to access *i*,*i*+4 and *i*,*i*+7 guanidinium staples in good yield and purity, and its application to helically constrain peptide sequences. We also report the careful evaluation of the interactions between the resulting cyclic peptides with three protein targets of interest (RNase S-protein, ubiquitin ligase hDM2 and the retinoic acid receptor-α (RARα)) including X-ray structure determination of several peptide-protein complexes.

Results and Discussion

The general SPS route to guanidinium stapled peptides is shown in Figure 2a. It was first optimized for the formation of a (*i*,*i*+4) staple using the sequence of the RNase S-peptide (**S-15**) where the His12 and Met13 residues were mutated to Ala for ease of synthesis and two suitably protected lysyl residues introduced at positions 6 and 10 for cyclization (**1**, Figure 2 and Table 1). The synthesis route features a selective deprotection of the Alloc-protected amine side chain and its thioacylation with Fmoc isothiocyanate (Fmoc-NCS) to form the corresponding Fmoc-activated thiourea prior to selective removal of the Mtt group on the second amine side chain. A number of reagents and conditions were tested and compared to promote the on-resin macrocyclization, via desulfurization and subsequent guanidinylation of the in situ generated carbodiimide intermediate.[16] These include mercury(II) chloride,[18] 1-ethyl-3-(3-dimethylaminopropyl)carbodiimide hydrochloride (EDC),[19] diisopropylcarbodiimide (DIC),[20] 2-chloro-1-

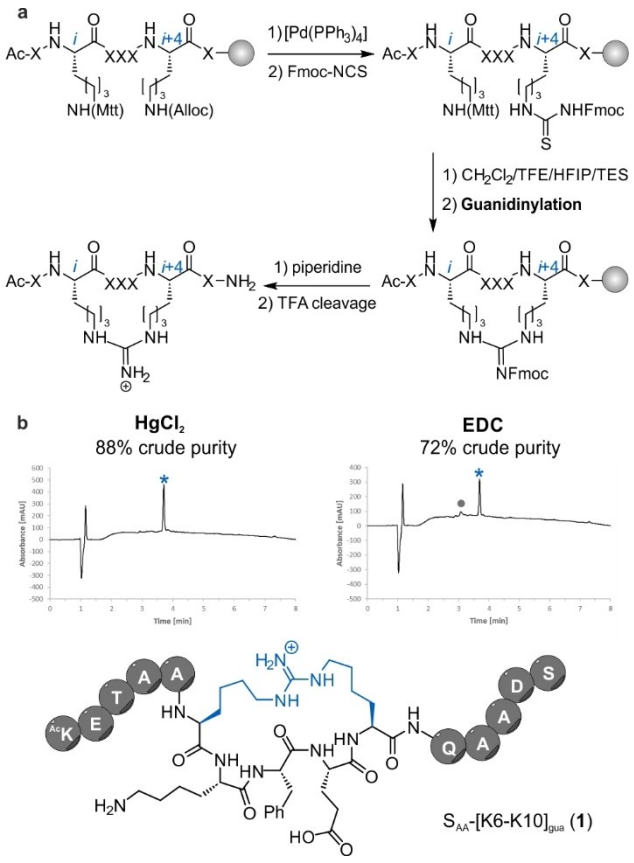

Figure 2. (a) General SPS route to guanidinium stapled peptides. TFE: 2,2,2-trifluoroethanol, HFIP: Hexafluoro-2-propanol, TES: Triethylsilane. (b) Comparison of the HPLC profiles of crude S_{AA}-[K6-K10]$_{gua}$ (**1**) after final cleavage from the resin (10–100% MeCN in H_2O with 0.1% TFA, 10 min, λ = 214 nm). The macrocyclization step was performed using 1.2 eq. of the guanidinylating agent indicated in bold (reacting at r.t. for 3 h and repeated overnight). On the chromatograms, the blue star shows the guanidine stapled compound and the grey dot the remaining thiourea derivative.

Table 1: List of stapled compounds from the RNase S-15, PMI and NCOA1-2 peptide sequences.

	Peptide sequences[a]		Yield
S-15		Ac-KETAAAKFERQHMDS-NH_2	
1	S_{AA}-[K6-K10]$_{gua}$	Ac-KETAA**X_2**KFE **X_1**Q**AA**DS-NH_2	10%
2	S-[K6-K10]$_{gua}$	Ac-KETAA**X_2**KFE**X_1**QHMDS-NH_2	10%
3	S-[O6-O10]$_{gua}$	Ac-KETAA**X_2**KFE**X_1**QHMDS-NH_2	24%
4	S-[K7-K10]$_{gua}$	Ac-KETAAA**X_2**FE**X_1**QHMDS-NH_2	16%
5	S-[K2-K6]$_{gua}$	Ac-K**X_2**TAA **X_1**KFERQHMDS-NH_2	17%
6	S-[K_D3-K10]$_{gua}$	Ac-KE**X_1**AAAKFE**X_2**QHMDS-NH_2	16%
7	S-[K3-O*10]$_{gua}$[b]	Ac-KE**X_2**AAAKFE**X_1**QHMDS-NH_2	nd
8	S-[K_D*2-O10]$_{gua}$[c]	Ac-K**X_1**TAAAKFE**X_2**QHMDS-NH_2	7%
PMI-N8A		Ac-TSFAEYWALLSP-NH_2	
9	PMI-[K4-K8]$_{gua}$	Ac-TSF**X_2**EYW**X_1**LLSP-NH_2	13%
10	PMI-[K_D4-K11]$_{gua}$	Ac-TSF**X_1**EYWALL**X_2**P-NH_2	12%
11	PMI-[K4-K11]$_{gua}$	Ac-TSF**X_2**EYWALL**X_1**P-NH_2	5%
NCOA1-2		Ac-RHKILHRLLQEGS-NH_2	
12	NCOA-[K3-K7]$_{gua}$	Ac-RH**X_2**ILH**X_1**LLQEGS-NH_2	13%
13	NCOA-[K4-K8]$_{gua}$	Ac-RHK**X_2**LHR**X_1**LQEGS-NH_2	24%
14	NCOA-[K6-K10]$_{gua}$	Ac-RHKIL**X_2**RLL**X_1**EGS-NH_2	19%

[a] The names of the compounds specify the stapled sites between squared brackets via the one-letter code of the amino acid side-chain used for the macrocyclization. In the linear sequence of the peptide, **X_1** indicates the Alloc-protected residue and **X_2** the Mtt-protected residue. [b] O* = Orn side chain coupled to Gly residue. [c] K* = Lys side chain coupled to Gly residue.

methylpyridinium iodide (Mukaiyama's reagent),[21] *N*-iodosuccinimide (NIS)[22] and iodine.[23] In each case, the reaction was performed at r.t. for 3 h in the presence of 1.2 eq. of the guanidinylating reagent and *N*,*N*-diisopropylethylamine (DIEA) as a tertiary base in CH_2Cl_2, or in a mixture of CH_2Cl_2 and *N*-methyl pyrrolidine (NMP) in the case of the $HgCl_2$ for solubility reason. DMF was generally avoided as some partial deprotection of the Fmoc-thiourea leading to incomplete conversion was observed during the macrocyclization step. The progress of the reaction was monitored by reversed phase HPLC and LC–MS analysis, and the guanidinylation step repeated overnight if the conversion was not completed. In each case, the purity of the crude compound was determined by HPLC after Fmoc deprotection and final cleavage of the peptide from the resin (Figure 2b and S1). $HgCl_2$ showed the highest efficiency in terms of conversion (full conversion to the expected S_{AA}-[K6-K10]$_{gua}$ (**1**) was achieved in <3h) and crude purity (reaching 88% purity based on HPLC). However, the high toxicity of $HgCl_2$, the formation of insoluble mercury sulfide by-product and the need to wash the resin with thiophenol or other mercaptan derivatives may limit the use of this approach. An interesting alternative is EDC, which readily promotes macrocyclization and leads to a clean reaction profile with a purity of 72% after final peptide cleavage. In contrast, reaction with DIC resulted in poor conversion to the guanidinylated product, and prolonged reaction time led mainly to the Fmoc deprotection of the thiourea, preventing any further macrocyclization. Similarly, when using Mukaiyama's reagent, the desired product did not form and unwanted side reactions took place instead, the main by-product being the pyridinium derivative resulting from the reaction of the free amine with Mukaiyama's reagent. The soft Lewis acid NIS gave satisfactory results with a purity of the crude product of 58%, but incomplete conversions were observed even after repeating the guanidinylation reaction once more. Macrocyclization was next performed on the wild-type S-15 sequence (**2**, Table 1), resulting in similar high crude purity. This indicates that no side-reaction involving the His or Met side chain occurred during the process.

Next, using EDC to promote the macrocyclization step, we prepared a series of RNase S-peptide derived macrocycles by varying the size and position of the ring in the sequence (Table 1). Both Lys and Orn side chains are compatible with the (*i*,*i*+3/4) stapling (**2**–**5**), while the macrocyclization in (*i*,*i*+7/8) is facilitated by inverting the configuration of the residue *i* (**6**), or by extending the length of one of the two side chains by coupling the Alloc-deprotected amine to a Gly residue (**7**–**8**).

To evaluate the effect of the position and size of the macrocycle on the α-helix stabilization, we next analyzed this series of stapled peptides by circular dichroism (CD) (Figure 3a). In the wild-type sequence, the salt bridge formed between the Glu2 and Arg10 residues is known to be a stabilizing interaction contributing to the partial helical

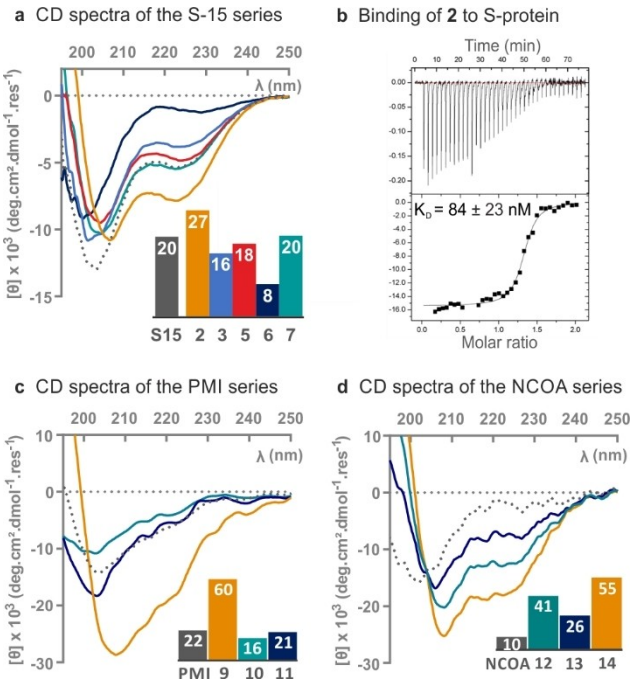

Figure 3. (a) CD spectra of linear S-15 (grey), and staples **2** (yellow), **3** (light blue), **5** (red), **6** (dark blue) and **7** (teal) in water at 50 μM, 3 °C. (b) ITC titrations of **2** (150 μM) into the S-protein (15 μM) in a Tris HCl 50 mM pH 8.0 buffer + 0.1 M NaCl + 3% glycerol. (c) CD spectra of linear PMI (grey), and staples **9** (yellow), **10** (teal) and **11** (dark blue) in water at 40 μM, 15 °C. (d) CD spectra of linear PMI (grey), and staples **12** (teal), **13** (dark blue) and **14** (yellow) in 15% TFE in water at 25 μM, 3 °C. The bar charts give percent helicity calculated from CD spectra $[\theta]_{222}$.[27]

folding of the peptide in solution.[24] The introduction of a guanidinium staple between the positions 6 and 10 (**2**), preserving the possibility for Glu2 to form a salt bridge with the constrained guanidinium, results in a substantial increase in α-helicity. Conversely, when Glu2 is mutated to form the (*i*,*i*+4) guanidinium macrocycle between positions 2 and 6 (**5**), the CD spectrum shows an α-helicity comparable to that of the linear peptide. The loss of the favorable salt bridge and charge-dipole interaction[25] therefore appears to be offset by the presence of the staple. Decreasing the size of the macrocycle, using Orn side chains for the (*i*,*i*+4) stapling, leads to reduced helicity (compare **2** and **3**), while for (*i*,*i*+7) stapling, extending the side chain by at least two additional atoms in the linker is necessary to be compatible with helical folding (compare **6** and **7**). Given the crucial role of Arg10 not only in mediating the intramolecular salt bridge but also in the interaction of the S-15 peptide with its partner S-protein to form the RNase-S complex,[26] we also assessed the binding affinity of the stapled peptide **2** in comparison to the unmodified native peptide using isothermal titration calorimetry (ITC). A strong interaction is still observed with the macrocyclic peptide (Figure 3b, S2 and Table S1), the constraint inducing a more favorable contribution to the binding entropy, which is however compensated by a reduced enthalpy.

To further expand our synthesis approach and investigate the influence of guanidinium stapling on the ability of α-peptides to bind protein surfaces and inhibit protein-protein interactions, we selected additional protein targets, i.e. hDM2 and Nuclear Hormone Receptors (NHR) for which peptide binders are known.

hDM2 is a ubiquitin ligase that prevents the action of the tumor suppressor p53 by interacting with a short α-helix at its N-terminal transactivation domain. The peptide PMI (TSFAEYWNLLSP) which has been identified by phage display as a potent inhibitor of this PPI,[28] able to bind to the same hDM2 hydrophobic cleft as p53, was used as the linear sequence of reference.[29] We introduced the guanidinium staple at the solvent exposed face of the PMI α-helix when bound to hDM2, to form either *i*,*i*+4 or *i*,*i*+7 macrocycles (Table 1, compounds **9**–**11**). The CD spectra of the three compounds show that only the short staple induces a significant increase in helicity in water, reaching 60 % of helical content, compared to 22 % for the linear sequence (Figure 3c). Next, the inhibition of the interactions between p53 and hDM2 and between p53 and hDMX (a closely-related regulatory protein but with a smaller hydrophobic pocket) was evaluated using a time resolved fluorescence energy transfer (TR-FRET) assay. The stapled peptides proved to be effective to disrupt the interaction of p53 with both hDM2 and hDMX partners, reaching more than 90 % inhibition at 100 nM (Figure S3). This requires, however, in the case of the (*i*,*i*+7) crosslink, that residue *i* be in the D-configuration. Subsequently, the dose-response curves were established for each compound (Figure 4a–b and S4–S7). The peptide having the short (*i*,*i*+4) crosslink (**9**), gave the best inhibition profile of the p53-hDM2 interaction (IC_{50} = 4.7 ± 0.2 nM), two-fold better than that obtained with PMI (IC_{50} = 9.4 ± 0.5 nM). This compound also showed high affinity for hDMX with an IC_{50} of 20 ± 0.9 nM, as does the compound **10**. The charged staple oriented toward the polar interface of the helix is thus well suited to lock the helical conformation while maintaining the main protein contacts responsible for tight binding. These inhibition profiles are similar or even slightly better compared to those reported for PMI peptides with hydrocarbon crosslinks at the same positions.[30]

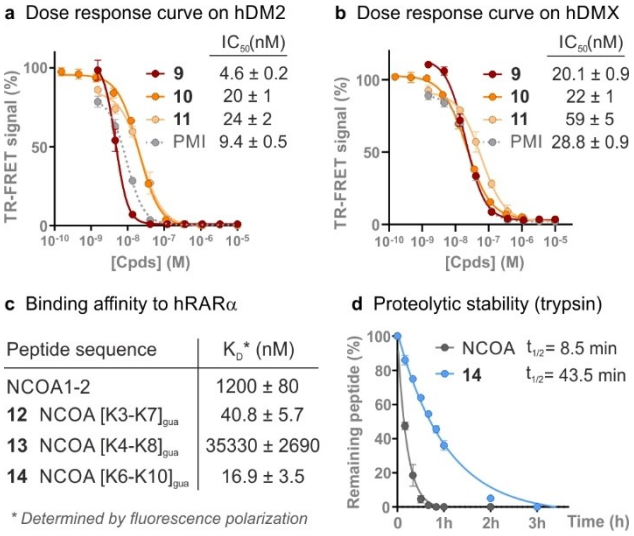

Figure 4. (a, b) Inhibition of the interaction between p53/hDM2 and p53/hDMX respectively, by compounds **9**–**11** assed by a TR-FRET assay. Data are presented as mean ± SD (duplicates) and IC_{50} values given ± SEM. (c) Binding affinities of compounds **12**–**14** to hRARα determined by a competitive fluorescence polarization assay. (d) Proteolytic stability of the guanidinium-stapled peptide **14** treated with trypsin, compared to the corresponding linear peptide NCOA1-2. The remaining peptide was quantified by HPLC, and the half-life ($t_{1/2}$) calculated using a non-linear one-phase decay.

NHR family members, such as the vitamin D receptor (VDR) or the retinoic acid receptor (RARα), are transcription factors whose activation requires the binding of their natural ligand as well as coactivators such as the nuclear receptor coactivators (NCOAs). NHRs also represent an important class of drug targets and disrupting the interaction between NHR and NCOA may be used to regulate the activity of these receptors for therapeutic applications.[31] This interaction is mediated by a consensus LXXLL motif contained in the helical binding domain of NCOA and we used the tridecapeptide NCOA1-2 as a basis to design (*i*,*i*+4) stapled peptides (Table 1, compounds **12**–**14**). Here, the guanidinium crosslink was placed at different positions to replace: either charged residues on the solvent-exposed face of the peptide (**12**), hydrophobic residues on the binding face (**13**) or polar residues at the edge of the binding site (**14**). All three stapled-peptides induce greater helicity than the linear sequence. Notably, the highest stabilization is obtained when the stapling positions replace polar residues, as seen with compounds **12** and **14**, which give 41 % and 55 % helix induction, respectively, compared to only 10 % for the linear sequence in 15 % TFE in water (Figure 3d). We performed then a probe-displacement assay

using the fluorescence polarization (FP) technique to measure the binding affinity of the compounds for hRARα (Figures 4c and S9). As expected, the polar guanidinium crosslink was poorly tolerated in a hydrophobic environment (K_D of 35 ± 2.7 μM for compound **13** compared to 1.2 ± 0.1 μM for the linear counterpart). On the other hand, compound **12** with the staple on the solvent-exposed face (K_D of 41 ± 5.7 nM) showed 25-fold higher affinity for RARα than NCOA1-2. The best result, however, was obtained for compound **14** with the staple on the edge of the binding site, which showed a 70-fold increase in binding strength, with a K_D of 17 ± 3.5 nM, suggesting that the staple itself may contribute to the interaction. Overall, the guanidinium macrocycles **12** and **14** gave binding affinities that were 5 to 15 times higher than their hydrocarbon counterparts (K_D of 654 nM and 75 nM respectively, as reported in the literature).[10b,32] This highlights the advantage of providing a charge to a staple placed in a polar environment. Compound **14** was further investigated in a proteolytic stability assay using trypsin, an enzyme that cleaves peptide bonds C-terminal to arginine or lysine residues. The results revealed a 5-fold increase in overall peptide stability compared to the linear sequence with half-lives ($t_{1/2}$) of 43.5 min vs 8.5 min respectively (Figure 4d and S11). Importantly, MS analysis confirmed the absence of cleavage at the guanidinium staple positions.

To gain precise insight into the conformation and the mode of binding of the guanidinium stapled peptides, we solved four representative co-crystal structures with each of the protein targets by X-ray diffraction. These include complexes between **4** and S-Protein (PDB ID: 9GF9, 1.8 Å resolution, Figure 5a), **9** and human hDM2 (PDB ID: 9GFC, 2.5 Å resolution, Figure 5b), **12** and liganded RARα (PDB ID: 9GFE, 1.6 Å resolution, Figure 5c), **14** and liganded RARα (PDB ID: 9GFI, 2.1 Å resolution, Figure 5d). In all four cases, the constrained peptide consistently adopts a regular α-helical structure, which superimposes well with that of the corresponding linear peptide, ensuring the preservation of key hydrophobic contacts with the protein surface. The electron density map of the guanidinium staples is generally well defined and revealed that the planar guanidinium moiety adopts a *cis/trans* conformation in most cases (Figure S10). Computational studies have shown that the *N*,*N*′-disubstituted guanidinium group can adopt two low-energy conformations: a *trans*/*trans* and a *cis*/*trans* conformation.[17a] Here, the constraint brought by the macrocycle with such a ring size (21 and 24 atoms) seems to favor the cis/*trans* conformation, at least in the crystal state. Only in the cocrystal of **4** and S-protein, which contains six symmetry independent molecules, both the *cis*/*trans* and the *trans*/*trans* conformations could be modelled in the electron density. Several additional and more specific features can be observed in the different structures. In the case of the RNase S-protein complex, the guanidinium staple proves to be an effective constrained mimic of the native Arg10 residue, preserving both the hydrogen bonding with the carbonyl oxygen of the protein backbone and the salt bridge with the Glu2 residue, further stabilizing the helical con-

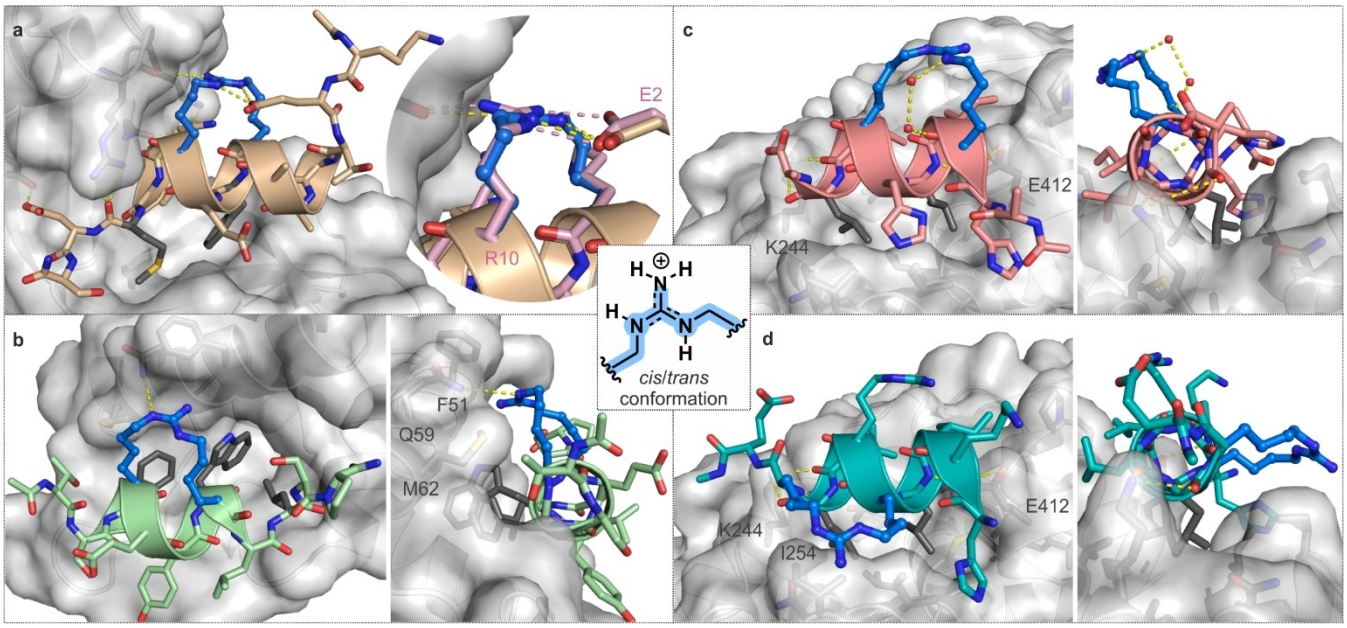

Figure 5. X-ray co-crystal structures of guanidinium stapled peptides in complex with proteins of interest. (a) On the left, crystal structure of **4** (wheat) in complex with the RNase S-protein. On the right, comparison of the H-bond interaction of the Arg10 residue in the native S-15 peptide sequence (pink, PDB ID: 2RNS) with the constrained guanidinium of the stapled peptide **4** in complex with the S-protein. (b) Crystal structure of **9** (green) in complex with human hDM2 (Views from the side and along the helical axis). (c) and (d) Crystal structures of respectively **12** (salmon) and **14** (teal) in complex with hRARα LBD-AM580 (Views from the side and along the helical axis). Both stapled peptides maintain the H-bond interactions with the charge clamp K244 and E412. Water molecules are represented as red spheres and H-bond as yellow dashes. Peptide residues located in protein hydrophobic pockets are colored in dark grey and the guanidinium staple in blue spheres in all structures.

formation of the peptide (Figure 5a). In the co-crystal structure involving the PMI-derived stapled peptide **9** and hDM2, the staple also contributes to the binding interaction through hydrogen bonding between the intracyclic guanidinium moiety and the Gln59 amide group, as well as through van der Waals contacts of the methylene groups of the staple with the Met62 side chain (Figure 5b). The proximity between the stapled guanidinium and the Phe51 aromatic ring makes a cation-pi interaction possible as well, even if the relative orientation of the two groups in the structure is not optimal. For the RARα LBD complexes, the key interactions of the LXXLL helix with the coactivator binding groove of RARα, including interactions with the charged clamp, are preserved (Figure 5c and 5d). Notably, the hydrogen bonds with Lys244 in helix 3 and with Glu412 in helix 12 of RARα are formed. It is noteworthy that in the **12**-RARα co-crystal structure where the guanidinium staple is solvent exposed, two well-defined H-bonded water molecules actually connect the peptide main chain to the guanidinium moiety and stabilize the macrocycle (Figure 5c). In the **14**-RARα complex, the guanidinium ring is oriented towards helix 4, and potentially exhibits increased flexibility as indicated by the less defined electronic density of the methylene groups (Figure 5d and S10). However, the guanidinium moiety is strategically positioned in close proximity to the side chain of Ile254, contributing to additional stabilization of the complex. Thus, an entropy gain and additional interactions may explain the significantly increased affinity of the stapled peptide **14** for RARα (vs NCOA1-2).

Conclusions

In conclusion, we have successfully developed a robust synthesis approach for the rapid generation of diverse arrays of guanidinium-stapled peptides on resin. This method relies on amino acids with orthogonally protected amino-functionalized side chains in the sequence, and benefits from their availability and diversity from commercial sources. Notably, it enables facile tuning of the staple properties (size, shape, and position of the guanidinium moiety in the ring) and of the secondary structure of the peptide. In several cases, the stapling strategy reported here led to peptides with tight – and in some cases significantly improved – binding to their respective protein target, confirming the potential of this approach. Structural studies of co-crystals with the proteins revealed that the stapled peptides studied consistently adopt a helical conformation upon protein binding with the disubstituted guanidinium displaying a defined and distinctive *cis*/*trans* geometry. Furthermore, our findings suggest that guanidinium staples can effectively mimic and constrain key arginine side chains engaged in specific interactions with the surface of a protein of interest. While our findings are promising, further studies are needed to globally assess the impact of guanidinium stapling on peptide resistance to degradation and cell permeability. Additionally, the versatility of our synthetic route suggests that it could be extended to prepare more intricate and diverse constrained peptides, such as sequences containing multiple guanidinium staples in a row or staples containing several intracyclic guanidinium moieties. Our ongoing efforts in these directions will be reported in due course.

Supporting Information

The data that support the findings of this study are available in the supplementary material of this article.

Acknowledgements

This research was supported in part by the Agence Nationale de la Recherche (ANR-15-CE07-0010, ANR-17-CE07-0020, and ANR-20-CE18-0038), the Conseil Régional de Nouvelle-Aquitaine (AAPR2021-2020-11969910). A CIFRE support from IMMUPHARMA BIOTECH SAS and ANRT to M.N. is gratefully acknowledged. M.P. and G.G. are grateful to Céline Reverdy, Cécile Planquette and Jean-Christophe Rain (Hybrigenics Services) for helpful discussions. This work has benefited from the facilities and expertise of IECB Biophysical and Structural Chemistry platform (BPCS), CNRS UMS3033, Inserm US001, Univ. Bordeaux. The authors thank the staff of Proxima 2 at the Soleil synchrotron for assistance in using the beamline.

Conflict of Interest

The authors declare no conflict of interest.

Data Availability Statement

The data that support the findings of this study are available in the supplementary material of this article.

Keywords: Stapled peptide · helix · guanidinium · solid-phase synthesis · protein-protein interaction

[1] a) C. Morrison, *Nat. Rev. Drug Discovery* **2018**, *17*, 531; b) A. A. Vinogradov, Y. Yin, H. Suga, *J. Am. Chem. Soc.* **2019**, *141*, 4167–4181; c) X. Ji, A. L. Nielsen, C. Heinis, *Angew. Chem. Int. Ed.* **2023**, *63*, e202308251.

[2] T. A. Hill, N. E. Shepherd, F. Diness, D. P. Fairlie, *Angew. Chem. Int. Ed.* **2014**, *53*, 13020.

[3] X. Li, S. Chen, W.-D. Zhang, H.-G. Hu, *Chem. Rev.* **2020**, *120*, 10079.

[4] a) K. Deyle, X.-D. Kong, C. Heinis, *Acc. Chem. Res.* **2017**, *50*, 1866; b) Y. Huang, M. M. Wiedmann, H. Suga, *Chem. Rev.* **2019**, *119*, 10360; c) C. Alleyne, R. P. Amin, B. Bhatt, E. Bianchi, J. C. Blain, N. Boyer, D. Branca, M. W. Embrey, S. N. Ha, K. Jette, D. G. Johns, A. D. Kerekes, K. A. Koeplinger, D. LaPlaca, N. Li, B. Murphy, P. Orth, A. Ricardo, S. Salowe, K. Seyb, A. Shahripour, J. R. Stringer, Y. Sun, R. Tracy, C. Wu, Y. Xiong, H. Youm, H. J. Zokian, T. J. Tucker, *J. Med. Chem.* **2020**, *63*, 13796; d) M. Tanada, M. Tamiya, A. Matsuo, A. Chiyoda, K. Takano, T. Ito, M. Irie, T. Kotake, R. Takeyama,

H. Kawada, R. Hayashi, S. Ishikawa, K. Nomura, N. Furuichi, Y. Morita, M. Kage, S. Hashimoto, K. Nii, H. Sase, K. Ohara, A. Ohta, S. Kuramoto, Y. Nishimura, H. Iikura, T. Shiraishi, *J. Am. Chem. Soc.* **2023**, *145*, 16610.

[5] a) D. P. Fairlie, A. Dantas de Araujo, *Pepide Sci.* **2016**, *106*, 843; b) L. Peraro, T. R. Siegert, J. A. Kritzer, in *Methods in Enzymology, Vol. 580* (Ed.: V. L. Pecoraro), Academic Press, **2016**, pp. 303–332.

[6] a) J. W. Taylor, *Biopolymers* **2002**, *66*, 49; b) R. S. Harrison, N. E. Shepherd, H. N. Hoang, G. Ruiz-Gomez, T. A. Hill, R. W. Driver, V. S. Desai, P. R. Young, G. Abbenante, D. P. Fairlie, *Proc. Natl. Acad. Sci. USA* **2010**, *107*, 11686.

[7] a) S. Cantel, C. Isaad Ale, M. Scrima, J. J. Levy, R. D. DiMarchi, P. Rovero, J. A. Halperin, A. M. D'Ursi, A. M. Papini, M. Chorev, *J. Org. Chem.* **2008**, *73*, 5663; b) Y. H. Lau, Y. Wu, M. Rossmann, B. X. Tan, P. de Andrade, Y. S. Tan, C. Verma, G. J. McKenzie, A. R. Venkitaraman, M. Hyvönen, D. R. Spring, *Angew. Chem. Int. Ed.* **2015**, *54*, 15410.

[8] G. Lautrette, F. Touti, H. G. Lee, P. Dai, B. L. Pentelute, *J. Am. Chem. Soc.* **2016**, *138*, 8340.

[9] a) C. E. Schafmeister, J. Po, G. L. Verdine, *J. Am. Chem. Soc.* **2000**, *122*, 5891; b) L. D. Walensky, G. H. Bird, *J. Med. Chem.* **2014**, *57*, 6275; c) P. M. Cromm, J. Spiegel, T. N. Grossmann, *ACS Chem. Biol.* **2015**, *10*, 1362.

[10] a) A. M. Ali, J. Atmaj, N. Van Oosterwijk, M. R. Groves, A. Dömling, *Comput. Struct. Biotechnol. J.* **2019**, *17*, 263; b) T. E. Speltz, S. W. Fanning, C. G. Mayne, C. Fowler, E. Tajkhorshid, G. L. Greene, T. W. Moore, *Angew. Chem. Int. Ed.* **2016**, *55*, 4252.

[11] a) Y. Tian, Y. Jiang, J. Li, D. Wang, H. Zhao, Z. Li, *ChemBioChem* **2017**, *18*, 2087; b) C. R. O. Bartling, F. Alexopoulou, S. Kuschert, Y. K. Y. Chin, X. Jia, V. Sereikaite, D. Özcelik, T. M. Jensen, P. Jain, M. M. Nygaard, K. Harpsøe, D. E. Gloriam, M. Mobli, K. Strømgaard, *J. Med. Chem.* **2023**, *66*, 3045.

[12] a) G. L. Verdine, G. J. Hilinski, in *Methods in Enzymology, Vol. Volume 503* (Eds.: K. D. Wittrup, L. V. Gregory), Academic Press, **2012**, pp. 3–33; b) G. H. Bird, E. Mazzola, K. Opoku-Nsiah, M. A. Lammert, M. Godes, D. S. Neuberg, L. D. Walensky, *Nat. Chem. Biol.* **2016**, *12*, 845; c) C. M. Fadzen, J. M. Wolfe, C.-F. Cho, E. A. Chiocca, S. E. Lawler, B. L. Pentelute, *J. Am. Chem. Soc.* **2017**, *139*, 15628; d) A. D. de Araujo, J. Lim, K.-C. Wu, H. N. Hoang, H. T. Nguyen, D. P. Fairlie, *RSC Chem. Biol.* **2022**, *3*, 895.

[13] a) F. Bernal, A. F. Tyler, S. J. Korsmeyer, L. D. Walensky, G. L. Verdine, *J. Am. Chem. Soc.* **2007**, *129*, 2456; b) T. N. Grossmann, J. T.-H. Yeh, B. R. Bowman, Q. Chu, R. E. Moellering, G. L. Verdine, *Proc. Natl. Acad. Sci. USA* **2012**, *109*, 17942; c) Q. Chu, R. E. Moellering, G. J. Hilinski, Y.-W. Kim, T. N. Grossmann, J. T. H. Yeh, G. L. Verdine, *MedChemComm* **2015**, *6*, 111.

[14] a) Y. H. Lau, P. de Andrade, S.-T. Quah, M. Rossmann, L. Laraia, N. Sköld, T. J. Sum, P. J. E. Rowling, T. L. Joseph, C. Verma, M. Hyvönen, L. S. Itzhaki, A. R. Venkitaraman, C. J. Brown, D. P. Lane, D. R. Spring, *Chem. Sci.* **2014**, *5*, 1804; b) L. Dietrich, B. Rathmer, K. Ewan, T. Bange, S. Heinrichs, T. C. Dale, D. Schade, T. N. Grossmann, *Cell Chem. Biol.* **2017**, *24*, 958–968.e955; c) T. E. Speltz, J. M. Danes, J. D. Stender, J. Frasor, T. W. Moore, *ACS Chem. Biol.* **2018**, *13*, 676; d) A. F. L. Schneider, J. Kallen, J. Ottl, P. C. Reid, S. Ripoche, S. Ruetz, T.-M. Stachyra, S. Hintermann, C. E. Dumelin, C. P. R. Hackenberger, A. L. Marzinzik, *RSC Chem. Biol.* **2021**, *2*, 1661.

[15] P. B. Crowley, A. Golovin, *Proteins* **2005**, *59*, 231.

[16] J. C. Manimala, E. V. Anslyn, *Eur. J. Org. Chem.* **2002**, *2002*, 3909.

[17] a) Y. Touati-Jallabe, L. Chiche, A. Hamzé, A. Aumelas, V. Lisowski, D. Berthomieu, J. Martinez, J.-F. Hernandez, *Chem. Eur. J.* **2011**, *17*, 2566; b) Y. Touati-Jallabe, E. Bojnik, B. Legrand, E. Mauchauffée, N. N. Chung, P. W. Schiller, S. Benyhe, M.-C. Averlant-Petit, J. Martinez, J.-F. Hernandez, *J. Med. Chem.* **2013**, *56*, 5964; c) A. Konieczny, M. Conrad, F. J. Ertl, J. Gleixner, A. O. Gattor, L. Grätz, M. F. Schmidt, E. Neu, A. H. C. Horn, D. Wifling, P. Gmeiner, T. Clark, H. Sticht, M. Keller, *J. Med. Chem.* **2021**, *64*, 16746; d) B. Li, H. Tang, A. Turlik, Z. Wan, X.-S. Xue, L. Li, X. Yang, J. Li, G. He, K. N. Houk, G. Chen, *Angew. Chem. Int. Ed.* **2021**, *60*, 6646.

[18] B. A. Linkletter, I. E. Szabo, T. C. Bruice, *J. Am. Chem. Soc.* **1999**, *121*, 3888.

[19] a) S. E. Schneider, P. A. Bishop, M. A. Salazar, O. A. Bishop, E. V. Anslyn, *Tetrahedron* **1998**, *54*, 15063; b) Z. Zhang, T. Carter, E. Fan, *Tetrahedron Lett.* **2003**, *44*, 3063.

[20] S. Robinson, E. J. Roskamp, *Tetrahedron* **1997**, *53*, 6697.

[21] a) Y. F. Yong, J. A. Kowalski, M. A. Lipton, *J. Org. Chem.* **1997**, *62*, 1540; b) Y. F. Yong, J. A. Kowalski, J. C. Thoen, M. A. Lipton, *Tetrahedron Lett.* **1999**, *40*, 53.

[22] K. Ohara, J.-J. Vasseur, M. Smietana, *Tetrahedron Lett.* **2009**, *50*, 1463.

[23] K. Skakuj, K. E. Bujold, C. A. Mirkin, *J. Am. Chem. Soc.* **2019**, *141*, 20171.

[24] J. J. Osterhout Jr., R. L. Baldwin, E. J. York, J. M. Stewart, H. J. Dyson, P. E. Wright, *Biochemistry* **1989**, *28*, 7059.

[25] K. R. Shoemaker, P. S. Kim, E. J. York, J. M. Stewart, R. L. Baldwin, *Nature* **1987**, *326*, 563.

[26] a) E. E. Kim, R. Varadarajan, H. W. Wyckoff, F. M. Richards, *Biochemistry* **1992**, *31*, 12304; b) M. P. Luitz, R. Bomblies, M. Zacharias, *Biophys. J.* **2017**, *113*, 1466.

[27] N. E. Shepherd, H. N. Hoang, G. Abbenante, D. P. Fairlie, *J. Am. Chem. Soc.* **2005**, *127*, 2974.

[28] M. Pazgier, M. Liu, G. Zou, W. Yuan, C. Li, C. Li, J. Li, J. Monbo, D. Zella, S. G. Tarasov, W. Lu, *Proc. Natl. Acad. Sci. USA* **2009**, *106*, 4665.

[29] C. Li, M. Pazgier, C. Li, W. Yuan, M. Liu, G. Wei, W.-Y. Lu, W. Lu, *J. Mol. Biol.* **2010**, *398*, 200.

[30] C. J. Brown, S. T. Quah, J. Jong, A. M. Goh, P. C. Chiam, K. H. Khoo, M. L. Choong, M. A. Lee, L. Yurlova, K. Zolghadr, T. L. Joseph, C. S. Verma, D. P. Lane, *ACS Chem. Biol.* **2013**, *8*, 506–512.

[31] a) J. Xu, R. C. Wu, B. W. O'Malley, *Nat. Rev. Cancer* **2009**, *9*, 615; b) K. J. Skowron, K. Booker, C. Cheng, S. Creed, B. P. David, P. R. Lazzara, A. Lian, Z. Siddiqui, T. E. Speltz, T. W. Moore, *Mol. Cell. Endocrinol.* **2019**, *493*, 110471.

[32] C. Phillips, L. R. Roberts, M. Schade, R. Bazin, A. Bent, N. L. Davies, R. Moore, A. D. Pannifer, A. R. Pickford, S. H. Prior, C. M. Read, A. Scott, D. G. Brown, B. Xu, S. L. Irving, *J. Am. Chem. Soc.* **2011**, *133*, 9696.

Manuscript received: August 26, 2024
Accepted manuscript online: December 23, 2024
Version of record online: January 13, 2025